Systematic evaluation of three porcine-derived collagen membranes for guided bone regeneration

Andrew Tai[1,2,#], Euphemie Landao-Bassonga[1,2,#], Ziming Chen[1,#], Minh Tran[3], Brent Allan[1, 3, 4], Rui Ruan[1], Dax Calder[3], Mithran Goonewardene[3], Hien Ngo[3], Ming Hao Zheng[1,2,*]

Key Words:
barrier membrane; collagen membrane; dental implant; guided bone regeneration; immunogen

From the Contents

*Corresponding author:
Ming Hao Zheng, minghao.zheng@uwa.edu.au.

#Author equally.

ABSTRACT

Guided bone regeneration is one of the most common surgical treatment modalities performed when an additional alveolar bone is required to stabilize dental implants in partially and fully edentulous patients. The addition of a barrier membrane prevents non-osteogenic tissue invasion into the bone cavity, which is key to the success of guided bone regeneration. Barrier membranes can be broadly classified as non-resorbable or resorbable. In contrast to non-resorbable membranes, resorbable barrier membranes do not require a second surgical procedure for membrane removal. Commercially available resorbable barrier membranes are either synthetically manufactured or derived from xenogeneic collagen. Although collagen barrier membranes have become increasingly popular amongst clinicians, largely due to their superior handling qualities compared to other commercially available barrier membranes, there have been no studies to date that have compared commercially available porcine-derived collagen membranes with respect to surface topography, collagen fibril structure, physical barrier property, and immunogenic composition. This study evaluated three commercially available non-crosslinked porcine-derived collagen membranes (Striate+™, Bio-Gide® and Creos™ Xenoprotect). Scanning electron microscopy revealed similar collagen fibril distribution on both the rough and smooth sides of the membranes as well as the similar diameters of collagen fibrils. However, D-periodicity of the fibrillar collagen is significantly different among the membranes, with Striate+™ membrane having the closest D-periodicity to native collagen I. This suggests that there is less deformation of collagen during manufacturing process. All collagen membranes showed superior barrier property evidenced by blocking 0.2–16.4 µm beads passing through the membranes. To examine the immunogenic agents in these membranes, we examined the membranes for the presence of DNA and alpha-gal by immunohistochemistry. No alpha-gal or DNA was detected in any membranes. However, using a more sensitive detection method (real-time polymerase chain reaction), a relatively strong DNA signal was detected in Bio-Gide® membrane, but not Striate+™ and Creos™ Xenoprotect membranes. Our study concluded that these membranes are similar but not identical, probably due to the different ages and sources of porcine tissues, as well as different manufacturing processes. We recommend further studies to understand the clinical implications of these findings.

Introduction

Osseointegrated dental implants have revolutionized the field of dentistry for the treatment of edentulism. In instances where there is insufficient alveolar bone to provide initial stabilization of a dental implant, additional bone regeneration is required before placing an implant. Guided bone regeneration (GBR) is the most common and effective strategy to provide sufficient bone for the osseointegration of dental implants into the alveolar bone. Dahlin et al.[1] in 1988 first described GBR, based on the

hypothesis that different cells have differential migration rates toward the wound during healing. Initially, a cell-occlusive polytetrafluoroethylene or Teflon™ (DuPont) membrane was utilized, fibroblasts and other soft connective tissue cells were prevented from populating the wound area.[2] Since then, the use of a barrier membrane to exclude non-osteogenic tissue has become the gold standard for GBR, since rapidly proliferating epithelium and connective tissue interfere with the regeneration of bone surrounding the dental implants.

Natural and synthetic barrier membranes have been developed for GBR.[2-4] Natural barrier membranes are comprised of collagen or chitosan, whereas synthetic barrier membranes are made of aliphatic polyesters, primarily polytetrafluoroethylene, polylactic acid or poly-glycolic acid. Natural barrier membranes, in particular collagen membranes, are popular for GBR as their overall advantages include biocompatibility and are resorbable, which avoids a second surgery for membrane removal.[3] Natural membranes that are currently used for GBR and derived from porcine sources include Striate+™, Bio-Gide® and Creos™ Xenoprotect, all of which are not cross-linked and manufactured using different protocols.

Collagen is a natural polymer that has been used in medical application for the last 100 years. There are seven types of fibrillar collagens (types I, II, III, V, XI, XXIV and XXVII), which are characterised by the repeating amino acid motif $(Gly-X-Y)_n$, with proline and 4-hydroxyproline amino acids commonly detected at the X and Y positions respectively.[5-8] The glycine residue is important for the stabilization of collagen. The tropocollagen molecules form triple helices by hydrogen bond formation between molecules and form a triple helix rod approximately 300 nm long and 1.5 nm in diameter.[9] Collagen fibrils are assembled from collagen rods from 50 to a few hundred nanometers in diameter depending on the types and number of collagen helix rods.

The D-periodicity of collagen fibrils is measured from overlap and gap regions between self-assembled collagen molecules. The D-periodicity of collagen fibrils is 67 nm, predicted by the Hodge-Petruska model[5, 9-11] and vadalited in different tissues.[12] Non-fibrillar collagens are also rich in glycine, proline and hydroxyproline, but the helical region is short or interrupted. They contribute to the formation of extracellular matrix's network, e.g., basement membrane. The commercially available porcine-derived membranes for GBR are mainly composed of fibrillar collagen types I and III. Processing of porcine-derived membranes can alter the D-periodicity of collagen fibrils.[13, 14] Alteration of the D-periodicity may affect the susceptibility to degradation mediated by collagenase which is present in saliva.[15, 16]

Implantation of xenogenic materials can cause acute immunological responses. A severe response could lead to poor bone regeneration affecting the osseointegration of dental implants. Common antigens in porcine barrier membranes are galactose-α-1,3-galactose (alpha-gal, α-gal)) and DNA. α-gal is a sugar molecule present in meat, including pork, beef and lamb. The enzyme α-1,3-galactosyltransferase is crucial for the synthesis of α-gal, but is only inactivated in humans and primates. Anti-α-gal antibodies (IgA, IgG, IgE and IgM), have been identified in humans and are responsible for triggering immune responses against porcine xenotransplants.[17] On the other hand, xenogeneic DNA, originating from the nucleus and mitochondria of the source tissue, can also trigger an immune reaction. Removal of DNA and α-gal in the manufacturing process is a key step for producing high quality animal or allogenic derived collagen devices.[18]

In this study, we examined the biological and physical barrier characteristics of three collagen membranes used for GBR that are all porcine-derived. Given the difference in the breed and age of animals as well as manufacturing processes, we hypothesized that there will be differences in the surface topology, diameter and D-periodicity of collagen fibrils, and α-gal and DNA content among these membranes. Our study has provided detailed analyses of the three porcine-derived collagen membranes - Creos™ Xenoprotect, Bio-Gide® and Striate+™ - and identified their similarities and differences, which we speculate may have clinical relevance with respect to the early wound healing events required for optimal peri-implant bone regeneration.

Methods

Collagen membranes

Three types of commercially-available porcine-derived collagen membranes: (1) Striate+™ manufactured by Orthocell Ltd., Perth, Western Australia, Australia (30 mm × 40 mm), (2) Bio-Gide® manufactured by Geistlich Pharma, Wolhusen, Switzerland (30 mm × 40 mm) and (3) Creos™ Xenoprotect manufactured by Matricel GmbH, Herzogenrath, Germany (30 mm × 40 mm) were used in this study. Raw materials are porcine mesentery as positive controls for heamatoxylin and eosin staining and real-time polymerase chain reaction (PCR), and porcine aortic valve (Boatshed Butcher at Cottesloe, Perth, Western Australia, Australia) is a positive control for DNA content and immunogenic porcine α-gal by immunohistochemistry analysis.

Scanning electron microscopy

Samples for scanning electron microscopy (SEM) imaging were cut to 3 mm × 3 mm and mounted on a stub. A layer of platinum was then sputtered onto the samples. Then the samples were imaged under 1555 VP-FESEM (Zeiss, Baden-Württemberg, Germany) at an accelerating voltage of 5 kV in the Centre for Microscopy, Characterization and Analysis, University of Western Australia. The D-periodcity and diameter of the collagen bundles were measured using FIJI ImageJ (64-bit Java1.8.0_172).[19] At least 11 images were analysed for each membrane. For determining the porosity

1 Centre for Orthopaedic Research, Faculty of Health and Medical Sciences, The University of Western Australia, Nedlands, Western Australia, Australia; 2 Perron Institute for Neurological and Translational Science, Nedlands, Western Australia, Australia; 3 UWA Dental School, The University of Western Australia, Nedlands, Western Australia, Australia; 4 Oral and Maxillofacial Department, St John of God Subiaco Hospital, Subiaco, Western Australia, Australia

of all three collagen membranes, SEM images (three images per membrane) depicting three types of membranes were imported into ImageJ software (v 1.53m; National Institutes of Health, Bethesda, MD, USA), where the porous regions of the images were identified and selected through threshold segmentation techniques based on their distinct gray values. The orientation of fibres was analysed by a Java plugin for ImageJ, OrientationJ.[20] Images of SEM were used for quantification of the diameter and D-periodicity of the bundles. The diameter and D-periodicity of collagen bundles were measured by ImageJ. The D-periodicity of collagen fibrils measured by the repeating pattern of gap and overlap regions. The diameter of the bundles was determined by measuring the distance between the top and bottom of the bundles.

Micro-computed tomography

Samples were stained overnight with iodine Lugol solution (Sigma-Aldrich, St. Louis, MO, USA). All three samples (Striate+™, Bio-Gide®, Creos™ Xenoprotect membranes) were mounted together in a polypropylene tube and then scanned by using Nikon XT H 225 ST CT, Inspect-X version (Nikon, Tokyo, Japan) at 47 kV, 117 μA, power 5.5 W, with a resolution of 12 mm in three dimensions. Totally, three membranes of each brand were used for measurement. Samples were reconstructed with computed tomography Pro 3D Version. The thickness of the collagen membranes was measured using AVIZO software (v2022.1; Thermo Fisher, Waltham, MA, USA).

Determination of barrier property of collagen membranes

Measurement of the barrier properties of collagen membranes was performed by gravity-based filtration. Striate+™, Bio-Gide®, Creos™ Xenoprotect membranes, Whatman Filter paper Grade 1 and Whatman Filter paper Grade 5 (Whatman International Ltd., Maidstone, UK) were trimmed to 3 cm × 3 cm and placed into 3D printed funnels as filters. Standard beads (PPS-6K & NFPPS-52-4K, Spherotech Inc., Lake Forest, CA, USA) of different sizes and concentrations (0.22 and 0.45 μm at 1:20 concentration; 0.88, 1.25, 2.0, 3.3, 5.2, 7.88, 10.1 and 16.4 μm at 1:50 concentration) were mixed and slowly filtered (**Additional Figure 1**). Filtrates were collected and analyzed by flow cytometry (BD LSRFortessa, BD Life Sciences, San Jose, CA, USA). Samples were acquired for 30 seconds at high speed with 60 μL/min. FSC (voltage: 709) and SSC (voltage: 412) settings were used for small size beads (PPS-6K, 0.22–1.25 μm) and FSC (voltage: 418) and SSC (voltage: 247) setting for large size beads (NFPPS-52-4K, 2.0–16.4 μm). Additionally, control measurements were also performed with mixed standard beads before filtration. Data were analyzed by FlowJo™ v10 Software (BD Life Sciences) and GraphPad Prism (v8.0.1, GraphPad Software, San Diego, CA, USA, www.graphpad.com). At least three membranes of each brand were used for the filtration assay.

Determination of cell nuclei remnants by real-time polymerase chain reaction

DNA (total 100 μL) extracted from the collagen membranes (Striate+™, Bio-Gide®, and Creos™ Xenoprotect) of the same weight (0.082 g) were purified by DNeasy Mericon Food Kit (Qiagen, Hilden, Germany). Totally, four samples of each type of membrane were used for the real-time PCR. DNA was also extracted from the porcine mesentery. The same volume (2 μL) of the purified DNA samples from membranes was analysed by real-time PCR using iTaq™ Universal SYBR® Green Supermix (Bio-Rad, Hercules, CA, USA) and the published primers (PPA6-forward: 5′-CTA CCT ATT GTC ACC TTA GTT-3′& reverse: 5′-GAG ATT GTG CGG TTA TTA ATG-3′) (IDT Technology Ltd., Coralville, IA, USA) for detection of porcine DNA, by targeting porcine mitochondrial specific gene (mtATP6).[21] Technical triplicate was applied to each sample.

Determination of cell nuclei remnants by histological analysis

Paraffin sections of the three commercial membranes were stained with heamatoxylin and eosin (Sigma-Aldrich) according to a standard protocol and imaged under light microscope (Zeiss) at a range of objective magnifications.

Determination of DNA content and porcine α-gal immunohistochemistry analysis

Positive control sample (porcine aortic valve, Boatshed Butcher at Cottesloe, Perth, Western Australia, Australia) and the collagen membranes were embedded in OCT solution, frozen by immersion in iso-pentane cooled with liquid-N2 and stored at 80℃ until required. Sections were prepared on a cryomicrotome at 10 μm thickness and placed on sialinated glass slides. Tissue sections were fixed by immersing them in pre-cooled acetone (–20℃) for 10 minutes, then washed twice with 1× phosphate buffered saline for 5 minutes each following by incubation with 0.1% Triton X for 5 minutes. Section were washed twice with 1× phosphate buffered saline for 5 minutes each and blocked with 3% bovine serum albumin. Sections were incubated with anti-DNA (1:1000, deposited by Voss, E.W., DSHB Hybridoma, Iowa City, IA, USA, RRID: AB_10805293) and anti-α-gal (1:1000, Isolectin GS-IB, Alexa Fluor 488 conjugate, Thermo Fisher, RRID: AB_2314662) at 4°C overnight. Sections stained with anti-DNA were then incubated with Alexa Fluor 680 donkey anti-mouse (1:500; RRID: AB_2762831, Thermo Fisher) at room temperature for 1 hour. After washing with 1× phosphate buffered saline three times, sections were stained with Hoechst 33342 (Thermo Fisher) and mounted with ProLong™ Diamond Antifade Mountant (Thermo Fisher). All sections were cover-slipped prior to imaging on a confocal laser scanning microscope (Nikon A1Si Confocal Microscope, Nikon, Tokyo, Japan).

Statistical analysis

Comparisons of multiple individual datasets were performed by one-way analysis of variance with Tukey's *post hoc* multiple comparison, after testing for the normal distribution of data. Statistical calculations were performed using GraphPad Prism software. The data are expressed as means ± standard error of mean (SEM), and we considered *P* values less than 0.05 as statistically significant.

Results

Surface topographic features of three collagen membranes

Resorbable collagen membranes (Creos™ Xenoprotect, Bio-Gide® and Striate+™) are derived from porcine tissue. In general, the membranes have a bilayer structure, with a rough and smooth side, which is a feature of the porcine source tissues. The smooth side refers to the side of the membrane with a relatively uniform surface and more parallel, aligned collagen bundles, while the rough side refers to the side with a porous, non-uniform surface with irregular collagen bundles. To understand the morphological differences between the collagen membranes, SEM was performed and images with different magnifications (364×, 19.75k×, 150k×) were selected and viewed in a side-by-side comparison. In all membranes, the smooth side had similar features, with no visible pores at 364× magnification (**Figure 1A**). At higher magnifications

(19.75 k× and 150 k×), clear fibrillar collagen bundles were noted in all membranes (**Figure 1A**). Striate+™ and Creos™ Xenoprotect exhibited a more uniform smooth side than Bio-Gide® as their peaks of fibre orientation distribution were closer to zero degrees determined by OrientationJ (**Figure 1A**). On the rough side, Creos™ Xenoprotect, Striate+™ and Bio-Gide® demonstrated the irregular distribution of fibre bundles throughout the rough side of the membranes (**Figure 1B**). The peaks of fibre orientation distribution of all the membranes were found to be further away from zero degrees meaning that the fibres tend not to be parallel. On the other hand, Striate+™ showed significantly smaller porosity than Bio-Gide® and Creos™ Xenoprotect at the smooth side analyzed by Image J (**Figure 1C**). There is no significant difference of porosity in smooth side between Bio-Gide® and Creos™ Xenoprotect. Also, there is no significant difference of porosity in rough side of all membranes (**Figure 1D**).
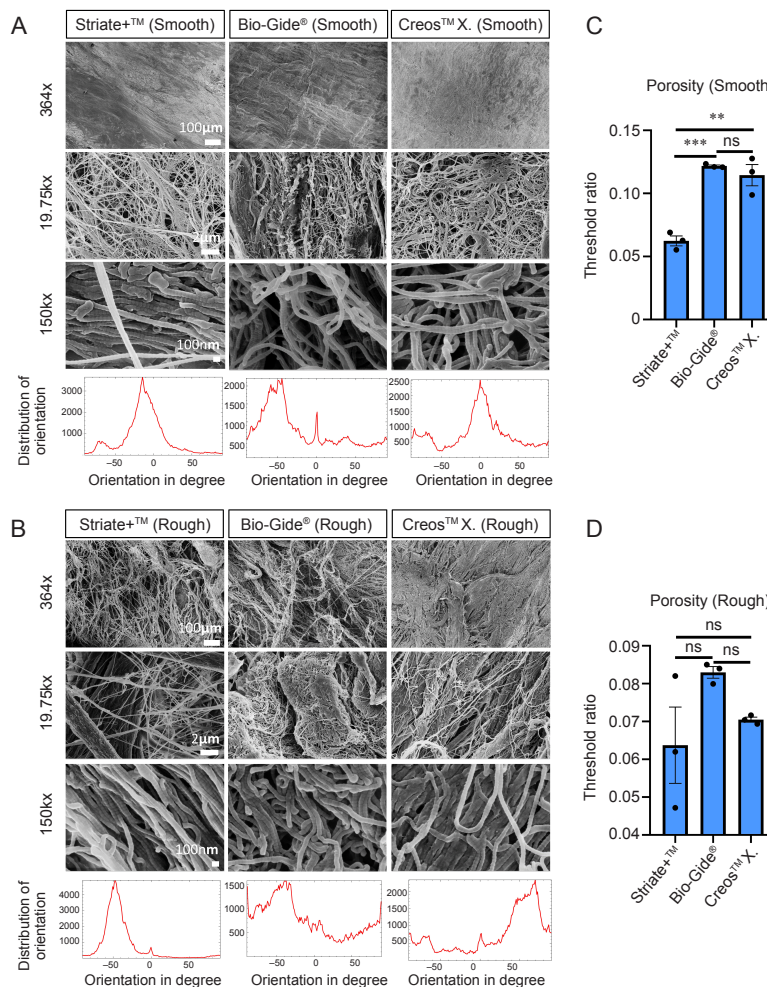

Figure 1. Scanning electron microscopy of porcine collagen membranes. (A, B) Smooth (A) and rough (B) sides of Striate+™, Bio-Gide® and Creos™ Xenoprotect. The smooth side of the collagen membranes showed a more uniform, smooth, and organized structure than the rough side. Scale bars: 100 μm (upper row), 2 μm (middle row), 100 nm (lower row). Representative scanning electron microscopy images of both smooth and rough sides of membranes at 150k× were analysed by OrientationJ for the orientation of fibres. Striate+™ and Creos™ Xenoprotect showed more uniform fibre orientation than Bio-Gide® on smooth side, whereas all three membranes showed random fibre orientation on rough side. (C, D) Porosity of smooth (C) and rough (D) sides of collagen membranes. Data are presented as means ± SEM. **$P < 0.01$, ***$P < 0.001$ (one-way analysis of variance with Tukey's *post hoc* multiple comparison). ns: no significance.

Diameter and D-periodicity of collagen fibrils in three collagen membranes

In addition to the surface topological analysis, the intrinsic properties of collagen fibrils, such as diameter and D-periodicity in the three collagen membranes were examined, as these parameters are affected in the manufacturing process. SEM results showed there was no significant difference in fibril diameter among three membranes: Striate+™, Bio-Gide® and Creos™ Xenoprotect (**Figure 2A**). However, the D-periodicity of collagen fibrils in Striate+™ membrane was higher than those in Bio-Gide® and Creos™ Xenoprotect . The D-periodicity of collagen bundles of Striate+™, membrane is closest to the native one (67 nm). There was no significant difference in D-periodicity between Bio-Gide® and -Creos™ Xenoprotect (**Figure 2B**).
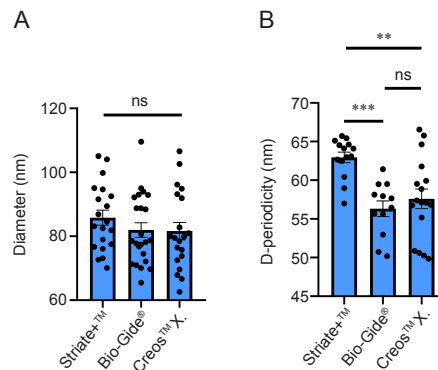

Figure 2. (A, B) Diameter (A) and D-periodicity (B) of collagen bundles in Striate+™, Bio-Gide® and Creos™ Xenoprotect (Creos™ X.). Data are presented as means ± SEM. **$P < 0.01$, ***$P < 0.001$ (one-way analysis of variance with Tukey's *post hoc* multiple comparison). ns: no significance.

Thickness of the collagen membranes in three collagen membranes

To determine the thickness of the collagen membranes, micro-computed tomography was used to scan through the collagen membranes (**Figure 3A**). Membranes were oriented so that cross-sections were obtained (**Figure 3B**). Bio-Gide® membrane is the thickest membrane, while Striate™ is the thinnest one (**Figure 3C**).
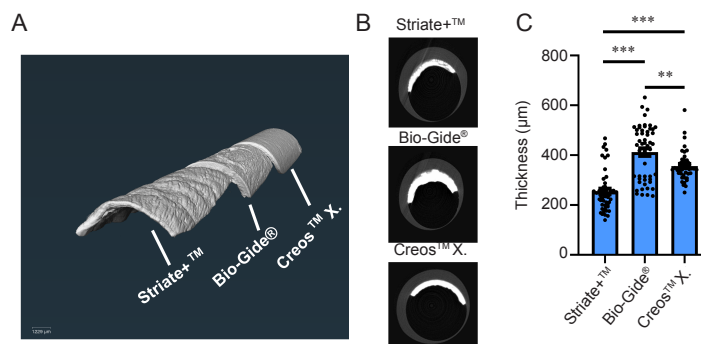
Figure 3. Thickness of porcine collagen membranes measured by micro-computed tomography. (A) Iodine-stained Striate+™, Bio-Gide® and Creos™ Xenoprotect (Creos™ X.) membranes were aligned in polypropylene tubes and scanned by micro-computed tomography. (B) Cross sections of Striate+™, Bio-Gide® and Creos™ Xenoprotect membranes were extracted by AVIZO software. (C) Thickness of three samples of each membrane. Data are presented as means ± SEM. At least 11 measurements were done on each membrane. **$P < 0.01$, ***$P < 0.001$ (one-way analysis of variance with Tukey's *post hoc* multiple comparison). ns: no significance.

Barrier property of three collagen membranes

To evaluate the barrier properties of the collagen membranes, beads of different sizes were used to mimic fibroblasts and other soft connective tissue cells with a range of cell size in the socket cavity. Using a gravity-based filtration method, all collagen membranes showed superior barrier property by blocking the passage of all bead sizes (0.22–16.4 μm; **Figure 4A–C**), while grades 1 and 5 Whatman filter papers did not block 0.22, 0.45, 0.88 and 1.25 μm-sized beads (**Figure 4A and B**).

DNA contents and immunogens in three collagen membranes

Our previous study reported that several collagen scaffolds widely used for rotator cuff tendon repairs contain cellular/DNA components, which may be responsible for the severe

immune rejection reactions.[18] To determine if the three collagen membranes contain DNA and α-gal, we performed histology, immunohistochemical detection (for α-gal and double stranded DNA) and real-time PCR-based mitochondrial DNA assay. All collagen membranes showed eosin-stained collagen fibres in the histological evaluation. Basophilic nuclear staining with heamatoxylin was only present in the raw materials (porcine mesentery) but was not detectable in any of the commercial collagen membranes (**Figure 5**). By immunostaining using anti-DNA immunostaining and Hoechst nuclear staining, the positive control, aorta valve was shown positive staining in the nuclei (**Figure 6**). No immunostaining signal was detected in any commercial membranes. Next, we utilized a more sensitive method, real-time PCR, to determine the unknown

DNA content in all membranes. The cycle threshold values of (0, 100 ng and 200 ng) porcine DNA and all membranes were plotted as a scatter plot shown in **Figure 7**. 0 ng porcine DNA, Striate+™ and Creos™ Xenoprotect showed high cycle threshold values at around 40 or beyond 40 detectable range, indicating that these two membranes have very few or no DNA contaminations. However, a relatively strong DNA signal (low cycle threshold) was detected in Bio-Gide® (1/50 portion of DNA extracted from 0.082 g membrane) similar to that of 100 ng porcine DNA (**Figure 7**).

Our anti-α-gal immunostaining analysis showed high α-gal expression in positive control porcine aorta, whereas all collagen membranes showed negative staining (**Figure 8**).
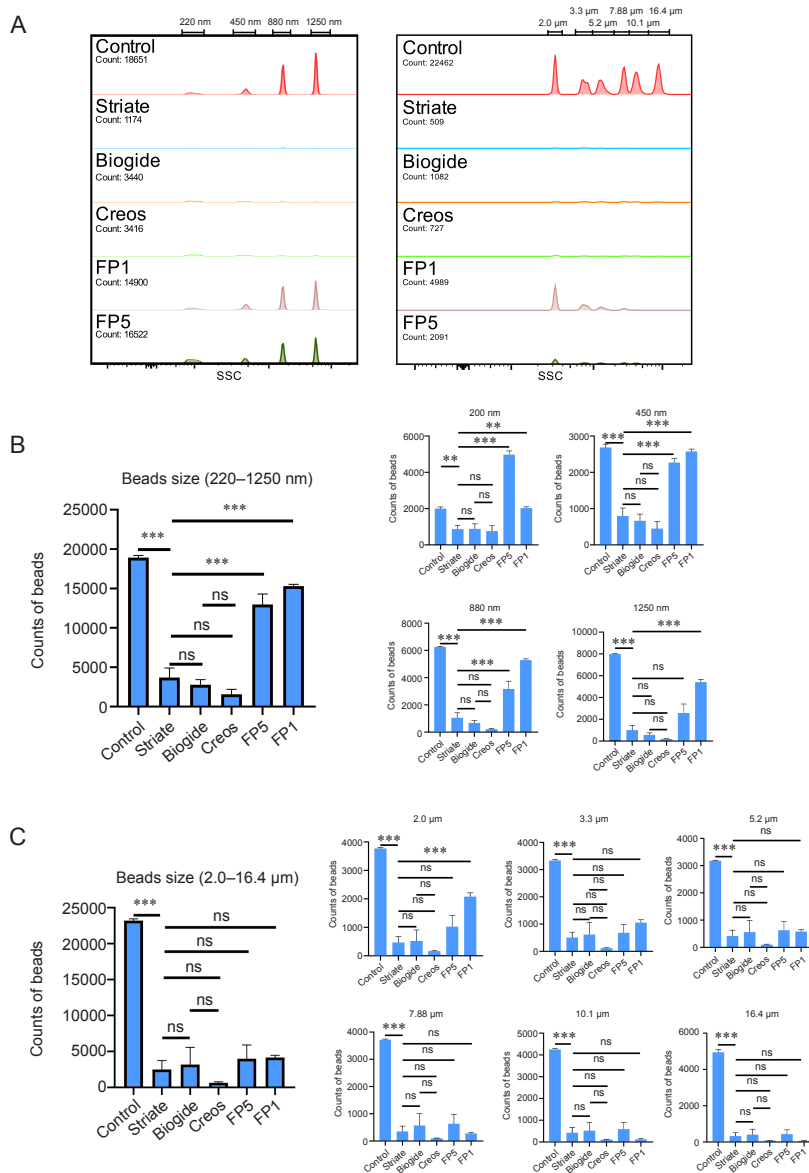

Figure 4. Barrier properties of three porcine collagen membranes measured by gravity-based filtration. (A) Representative results of collagen membranes' barrier property by filtration with mixed standard beads in different sizes. (B, C) Quantitative analysis of beads with all small (B, 220, 450, 880, and 1250 nm) and large (C, 2.0, 3.3, 5.2, 7.88, 10.1, and 16.4 μm) sizes passing through different collagen membranes. Data are presented as means ± SEM. **$P < 0.01$, ***$P < 0.001$ (one-way analysis of variance with Tukey's *post hoc* multiple comparison). FP1: Whatman Filter paper Grade 1; FP5: Whatman Filter paper Grade 5; ns: no significance.
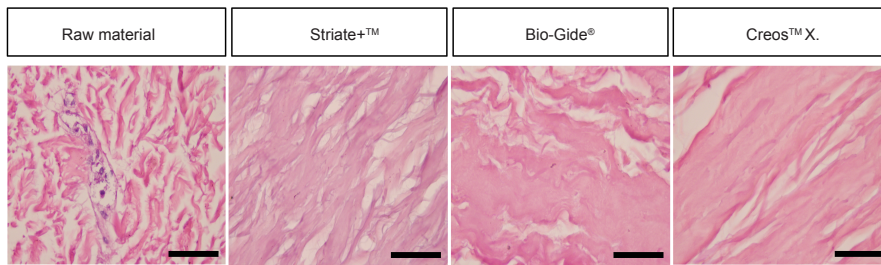
Figure 5. Heamatoxylin and eosin staining of different porcine collagen membranes. No heamatoxylin staining was found in all membranes. Scale bars: 50 μm. Creos™ X.: Creos™ Xenoprotect.
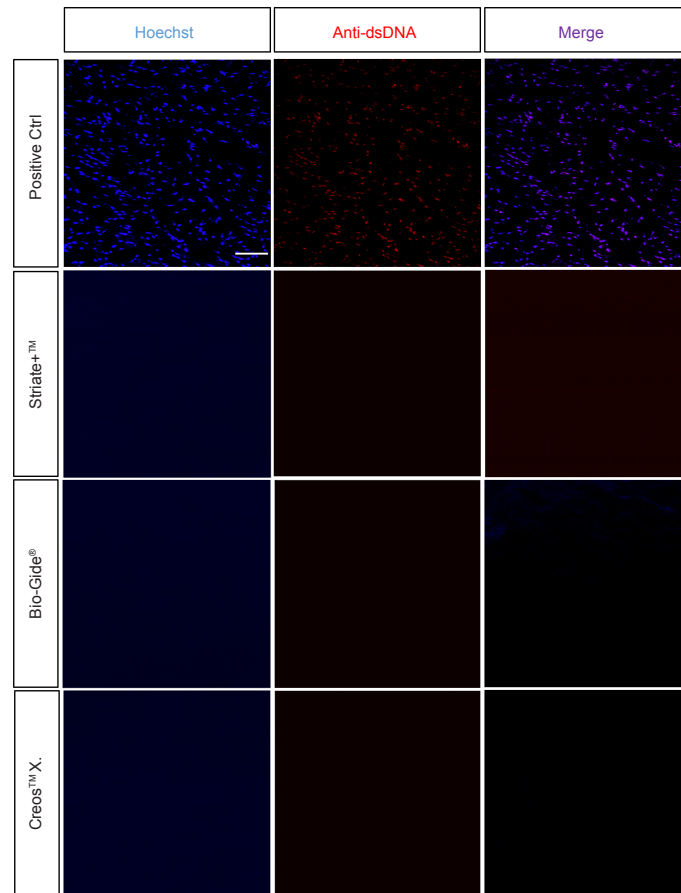
Figure 6. Anti-DNA immunostaining on different porcine collagen membranes. No DNA was found in all membranes by anti-DNA immunostaining. Positive control (Ctrl) indicates porcine aortic valve. Scale bar: 100 μm. Creos™ X.: Creos™ Xenoprotect; dsDNA: double stranded DNA.
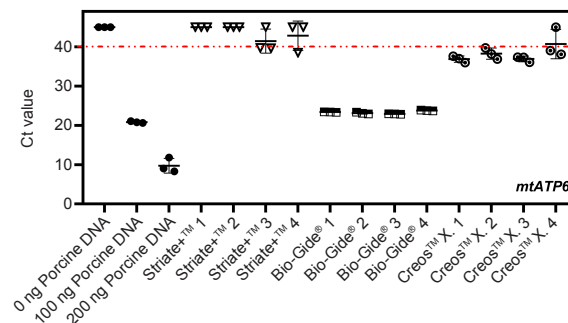
Figure 7. Determination of DNA content in different collagen membranes by real-time polymerase chain reaction. Among the three collagen membranes, only Bio-Gide® membrane showed significant DNA signal content. Data plotted above red dot line indicates undetectable within 40 cycles. Creos™ X.: Creos™ Xenoprotect; Ct: cycle threshold.
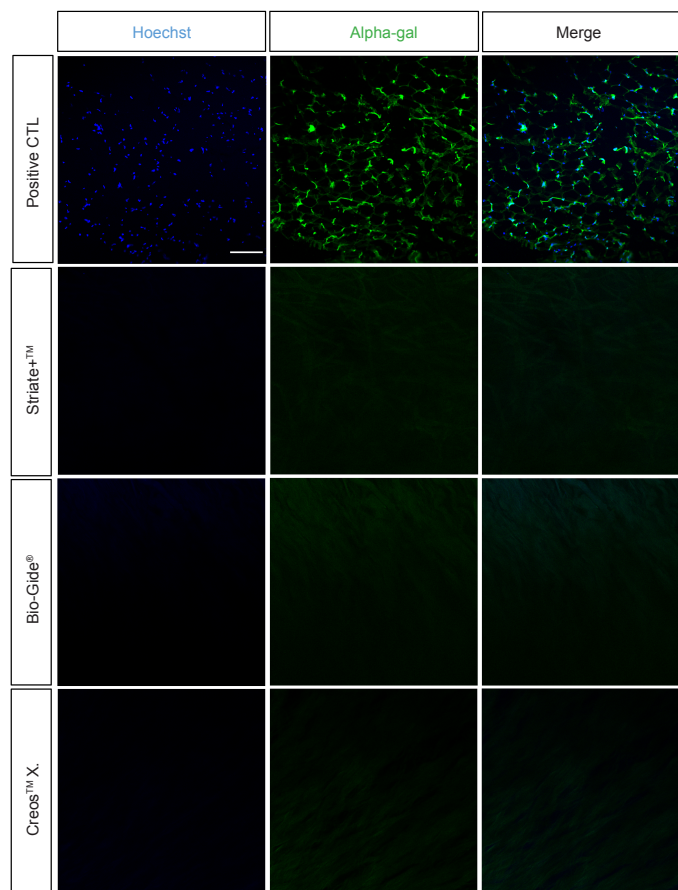
Figure 8. α-gal expression in different collagen membranes. No α-gal signal was detected in Creos™ Xenoprotect, Striate+™ and Bio-Gide® by anti-α-gal immunostaining. Positive control (Ctrl) indicates porcine aortic valve. Scale bar: 100 μm. α-gal: alpha-gal, galactose-α-1,3-galactose; Creos™ X.: Creos™ Xenoprotect.

Discussion

GBR is aided by the use of a barrier membrane to promote bone augmentation and osseointegration of dental implants. The barrier membrane prevents the growth of soft tissues into the wound to allow osteogenic cells to proliferate within the defect. Native collagen membranes (NCMs) have become popular as they are resorbed and degraded in-situ. NCMs can also promote soft tissue healing.[22] As NCMs are biodegradable, cross-linking of collagen membranes was developed to maintain the integrity and strength. However, a recent systematic review showed no difference in bone regeneration between cross-linked and resorbable collagen membranes.[23] Furthermore, cross-linked collagen membranes may impair soft tissue healing or cause wound infections.[24] Therefore, collagen barrier membranes without cross-linking have become widely used and studied.[3] The effective membrane for GBR must be able to act as a physical barrier against cell invasion but not inhibit bone regeneration on the other side of the membrane. NCMs must not contain immunogens which can cause severe immune reactions and result in poor bone regeneration, compromising the osseointegration of dental implants. This study is the first systematic examination of similar commercial native collagen membranes for GBR on their barrier properties, surface topological details, fibre diameter and D-periodicity, and immunogen contamination. We conclude that these membranes are not identical.

The surface topological examination focused on the distribution and density of collagen bundles in the three commercially available collagen membranes (Creos™ Xenoprotect, Bio-Gide® and Striate+™) by SEM. Our SEM analysis showed that all membranes have smooth and rough sides which can be easily distinguished from each other based on the density and distribution of collagen bundles. The smooth side of NCMs showed a high density of aligned collagen bundles, whereas the rough side showed relatively loose and irregular collagen bundles. At 364× magnification view, almost no pores were observed on the smooth surface of the collagen membranes. At 150k× magnification, most of the pores on both the smooth and rough side are smaller than 1 μm, which sufficiently prevent cells from passing through the membranes. In most cases, measurement of porosity was used to estimate their barrier property[25] probably due to the lack of an assay system. We designed an assay system using beads and gravity filtration as well as flow cytometry analysis. By using this assay system, all collagen membranes showed superior barrier property by gravity-based filtration, which is independent of the thickness of membranes, and thus explains why all the membranes can efficiently act as a physical barrier to prevent the in-growth of cells into the bone cavity.

The diameter of collagen fibrils is a result of the number and type of assembled collagen molecules, whereas the

D-periodicity of collagen fibrils is measured from overlap and gap regions between self-assembled collagen molecules. The diameter and D-peridocity of collagen fibrils in each of the three collagen membranes were measured by SEM at 150 k× magnification. No significant difference was found in the diameter of collagen fibrils between the three collagen membranes. Based on the 1.5 nm diameter of a mature collagen molecule,[9] approximately 54 tropocollagen molecules are self-assembled into collagen fibrils (81.62–85.82 nm in diameter) in these collagen membranes. The mean of D-periodocity of the collagen membranes Striate+™, Bio-Gide® and Creos™ Xenoprotect, were measured as 62.9, 56.3 m and 57.4 nm, respectively. Striate+™ showed the highest D-periodocity and is closest to the average D-periodicity of unprocessed natural collagen fibrils (67 nm)[5, 9-11] suggesting less deformation in the manufacturing process. The difference in the D-periodicity could be due to the origin of porcine tissues (age and/or tissue origin) and/or manufacture processing such as dehydration and compression.[13-15] Different D-periodicity of collagen fibrils does not affect the function as physical barriers which are mainly determined by the density and distribution of the collagen bundle, but it could affect their susceptibility to salivary collagenase.[15, 16] Furthermore, a recent study demonstrated that collagen membranes could be bio-inductive and facilitate the tissue repair.[26] GBR membranes have also been shown to have additional bone regenerative functions such as the triggering of expression of bone remodeling genes and differential concentration of bone morphogenetic protein-2 on the membrane surface.[27] Furthermore, a study suggested that collagen membranes may have an intrinsic transforming growth factor-β activity which may affect the tissue regeneration process.[28] It remains unclear whether maintenance of native superstructure of collagen fibrils such as D-periodicity could be important for bone and/or soft tissue regeneration during GBR or other tissue regenerations. As D-periodicity may also affect the susceptibility to collagenase degradation in saliva,[15, 16] the stability of all the membranes remains to be addressed.

Porcine small intestine submucosa, a collagen-rich tissue, has been used to manufacture collagen scaffolds for tissue regeneration. However, the immunogenic substances such as DNA present in small intestine submucosa can cause severe immunological reactions after implantation in the human body.[18] The removal of α-gal in collagen-based medical devices is important to prevent immunological rejection, especially in people with α-gal syndrome.[29, 30] These major immunogenic substances have to be removed during manufacturing of the collagen membranes. To test whether there was any immunogenic substance in the porcine-derived collagen membranes, we measured the DNA and α-gal content in the three porcine-derived collagen membranes by heamatoxylin and eosin staining, immunostaining and PCR. No α-gal and DNA, including nuclear remnants, were detected in any of the membranes by immunostaining and Hoechst staining. However, using real-time PCR, a relatively strong DNA signal was observed in the Bio-Gide® membrane but not in Creos™ Xenoprotect and Striate+™ membranes. The cycle threshold value of porcine specific gene (*mtATP6*) from Bio-Gide®

membranes is similar to that of 100 ng porcine DNA. This could be possibly due to insufficient removal of immunogens during the manufacture of the Bio-Gide® membranes. Our data may explain why more inflammatory cells and cytokines were found in Bio-Gide® than another porcine collagen membrane in a recent study using a rat model.[25]

An ideal GBR membrane should include the following characteristics 1) good barrier property, 2) low immunogen content 3) good for soft tissue regeneration and 4) easy to handle. Our study has established robust assays for determining their barrier property and immunogenic content which are the key elements of GBR. The effects of the collagen membranes on soft and bone tissue regeneration have not been addressed which is also the limitation of this study. Further studies using animal GBR models can address both the extent of inflammation and tissue regeneration. On the other hand, the thickness of the membranes may potentially affect the quality of the surgical procedure. It appears to be more difficult to manipulate thicker membranes in GBR procedure. Rating by dentists could be a way to determine their handling experience. A more scientific assay system should be designed to address the handling property without bias.

In conclusion, our study showed that these three non-cross-linked membranes are similar but not identical, probably due to the different ages and sources of porcine tissues as well as different manufacturing processes. Striate+™ membrane is closest to the D-periodicity of natural, unprocessed collagen. Low residual DNA was detected in Bio-Gide® but not in Striate+™ and Creos™ Xenoprotect. All of these membranes have similar superior barrier properties. Further comparative studies are required to conclude their clinical outcomes.

Additional file
Additional Figure 1: Determination of barrier property of collagen membranes by gravity-based filtration.

1. Dahlin, C.; Linde, A.; Gottlow, J.; Nyman, S. Healing of bone defects by guided tissue regeneration. *Plast Reconstr Surg.* **1988**, *81*, 672-676.
2. Sasaki, J. I.; Abe, G. L.; Li, A.; Thongthai, P.; Tsuboi, R.; Kohno, T.;

Imazato, S. Barrier membranes for tissue regeneration in dentistry. *Biomater Investig Dent.* **2021**, *8*, 54-63.

3. Sbricoli, L.; Guazzo, R.; Annunziata, M.; Gobbato, L.; Bressan, E.; Nastri, L. Selection of collagen membranes for bone regeneration: a literature review. *Materials (Basel).* **2020**, *13*, 786.

4. Lee, S. W.; Kim, S. G. Membranes for the guided bone regeneration. *Maxillofac Plast Reconstr Surg.* **2014**, *36*, 239-246.

5. Kadler, K. E.; Holmes, D. F.; Trotter, J. A.; Chapman, J. A. Collagen fibril formation. *Biochem J.* **1996**, *316 (Pt 1)*, 1-11.

6. Pace, J. M.; Corrado, M.; Missero, C.; Byers, P. H. Identification, characterization and expression analysis of a new fibrillar collagen gene, COL27A1. *Matrix Biol.* **2003**, *22*, 3-14.

7. Boot-Handford, R. P.; Tuckwell, D. S.; Plumb, D. A.; Rock, C. F.; Poulsom, R. A novel and highly conserved collagen (pro(alpha)1(XXVII)) with a unique expression pattern and unusual molecular characteristics establishes a new clade within the vertebrate fibrillar collagen family. *J Biol Chem.* **2003**, *278*, 31067-31077.

8. Exposito, J. Y.; Valcourt, U.; Cluzel, C.; Lethias, C. The fibrillar collagen family. *Int J Mol Sci.* **2010**, *11*, 407-426.

9. Hodge, A. J.; Petruska, J. A. Recent studies with the electron microscope on ordered aggregates of the tropocollagen macromolecule. In *Aspects of Protein Structure, Ramachandran*, G. N., Ed. Academic Press: New York, 1963; pp 289-300.

10. Chapman, J. A.; Tzaphlidou, M.; Meek, K. M.; Kadler, K. E. The collagen fibril--a model system for studying the staining and fixation of a protein. *Electron Microsc Rev.* **1990**, *3*, 143-182.

11. Orgel, J. P.; Irving, T. C.; Miller, A.; Wess, T. J. Microfibrillar structure of type I collagen in situ. *Proc Natl Acad Sci U S A.* **2006**, *103*, 9001-9005.

12. Wallace, J. M.; Chen, Q.; Fang, M.; Erickson, B.; Orr, B. G.; Banaszak Holl, M. M. Type I collagen exists as a distribution of nanoscale morphologies in teeth, bones, and tendons. *Langmuir.* **2010**, *26*, 7349-7354.

13. Kemp, A. D.; Harding, C. C.; Cabral, W. A.; Marini, J. C.; Wallace, J. M. Effects of tissue hydration on nanoscale structural morphology and mechanics of individual type I collagen fibrils in the Brtl mouse model of Osteogenesis Imperfecta. *J Struct Biol.* **2012**, *180*, 428-438.

14. Wells, H. C.; Sizeland, K. H.; Kelly, S. J. R.; Kirby, N.; Hawley, A.; Mudie, S.; Haverkamp, R. G. Collagen fibril intermolecular spacing changes with 2-propanol: a mechanism for tissue stiffness. *ACS Biomater Sci Eng.* **2017**, *3*, 2524-2532.

15. Watanabe-Nakayama, T.; Itami, M.; Kodera, N.; Ando, T.; Konno, H. High-speed atomic force microscopy reveals strongly polarized movement of clostridial collagenase along collagen fibrils. *Sci Rep.* **2016**, *6*, 28975.

16. Uitto, V. J.; Suomalainen, K.; Sorsa, T. Salivary collagenase. Origin, characteristics and relationship to periodontal health. *J Periodontal Res.* **1990**, *25*, 135-142.

17. Hilger, C.; Fischer, J.; Wölbing, F.; Biedermann, T. Role and mechanism of galactose-alpha-1,3-galactose in the elicitation of delayed anaphylactic reactions to red meat. *Curr Allergy Asthma Rep.* **2019**, *19*, 3.

18. Zheng, M. H.; Chen, J.; Kirilak, Y.; Willers, C.; Xu, J.; Wood, D. Porcine small intestine submucosa (SIS) is not an acellular collagenous matrix and contains porcine DNA: possible implications in human implantation. *J Biomed Mater Res B Appl Biomater.* **2005**, *73*, 61-67.

19. Schneider, C. A.; Rasband, W. S.; Eliceiri, K. W. NIH Image to ImageJ: 25 years of image analysis. *Nat Methods.* **2012**, *9*, 671-675.

20. Rezakhaniha, R.; Agianniotis, A.; Schrauwen, J. T.; Griffa, A.; Sage, D.; Bouten, C. V.; van de Vosse, F. N.; Unser, M.; Stergiopulos, N. Experimental investigation of collagen waviness and orientation in the arterial adventitia using confocal laser scanning microscopy. *Biomech Model Mechanobiol.* **2012**, *11*, 461-473.

21. Yoshida, T.; Nomura, T.; Shinoda, N.; Kusama, T.; Kadowaki, K.; Sugiura, K. Development of PCR primers for the detection of porcine DNA in feed using mtATP6 as the target sequence. *Shokuhin Eiseigaku Zasshi.* **2009**, *50*, 89-92.

22. Zitzmann, N. U.; Naef, R.; Schärer, P. Resorbable versus nonresorbable membranes in combination with Bio-Oss for guided bone regeneration. *Int J Oral Maxillofac Implants.* **1997**, *12*, 844-852.

23. Jiménez Garcia, J.; Berghezan, S.; Caramês, J. M. M.; Dard, M. M.; Marques, D. N. S. Effect of cross-linked vs non-cross-linked collagen membranes on bone: A systematic review. *J Periodontal Res.* **2017**, *52*, 955-964.

24. Becker, J.; Al-Nawas, B.; Klein, M. O.; Schliephake, H.; Terheyden, H.; Schwarz, F. Use of a new cross-linked collagen membrane for the treatment of dehiscence-type defects at titanium implants: a prospective, randomized-controlled double-blinded clinical multicenter study. *Clin Oral Implants Res.* **2009**, *20*, 742-749.

25. Zhu, M.; Duan, B.; Hou, K.; Mao, L.; Wang, X. A comparative in vitro and in vivo study of porcine- and bovine-derived non-cross-linked collagen membranes. *J Biomed Mater Res B Appl Biomater.* **2023**, *111*, 568-578.

26. Chen, P.; Wang, A.; Haynes, W.; Landao-Bassonga, E.; Lee, C.; Ruan, R.; Breidahl, W.; Shiroud Heidari, B.; Mitchell, C. A.; Zheng, M. A bio-inductive collagen scaffold that supports human primary tendon-derived cell growth for rotator cuff repair. *J Orthop Translat.* **2021**, *31*, 91-101.

27. Elgali, I.; Omar, O.; Dahlin, C.; Thomsen, P. Guided bone regeneration: materials and biological mechanisms revisited. *Eur J Oral Sci.* **2017**, *125*, 315-337.

28. Panahipour, L.; Kargarpour, Z.; Luza, B.; Lee, J. S.; Gruber, R. TGF-β activity related to the use of collagen membranes: in vitro bioassays. *Int J Mol Sci.* **2020**, *21*, 6636.

29. Kuravi, K. V.; Sorrells, L. T.; Nellis, J. R.; Rahman, F.; Walters, A. H.; Matheny, R. G.; Choudhary, S. K.; Ayares, D. L.; Commins, S. P.; Bianchi, J. R.; Turek, J. W. Allergic response to medical products in patients with alpha-gal syndrome. *J Thorac Cardiovasc Surg.* **2022**, *164*, e411-e424.

30. Steinke, J. W.; Platts-Mills, T. A.; Commins, S. P. The alpha-gal story: lessons learned from connecting the dots. *J Allergy Clin Immunol.* **2015**, *135*, 589-596; quiz 597.